JOURNAL OF GEOPHYSICAL RESEARCH, VOL. 114, A08306, doi:10.1029/2008JA013957, 2009

Click Here for Full Article

Solar activity dependence of the topside ionosphere at low latitudes

Yiding Chen,[1,2] Libo Liu,[1] Weixing Wan,[1] Xinan Yue,[1] and Shin-Yi Su[3]

Received 1 December 2008; revised 28 May 2009; accepted 5 June 2009; published 22 August 2009.

[1] We investigated the solar activity dependence of the topside ionosphere with ROCSAT-1 observations. The distribution of the plasma density at 600 km altitude shows features with considerable local time, season, and solar activity differences. In the daytime, plasma density peaks around the dip equator. This peak is more distinct in equinoxes and weaker in May–July, and it enhances with solar activity in all seasons. The seasonal behavior of this peak is primarily controlled by the seasonal variations of neutral density and $\mathbf{E} \times \mathbf{B}$ vertical drift. The enhancement of the peak with solar activity is related to the effect of $\mathbf{E} \times \mathbf{B}$ vertical drift. Around sunset, double peaks are found in the latitudinal distribution of plasma density in solar maximum equinoxes and December solstice, which are mainly attributed to the effects of strong prereversal enhancement (PRE) vertical drift. Moreover, the plasma density at 600 km altitude strongly depends on the solar proxy $P = (F_{107} + F_{107A})/2$. At higher altitudes, e.g., 800 km, the amplification trend prevails in the solar activity variations of plasma density. In contrast, the plasma density at 600 km altitude presents three kinds of patterns (linear, amplification, and saturation), which has not been reported. Saturation effect is found at equinox sunset around the dip equator. This saturation effect is attributed to the increase in the PRE vertical drift with solar activity. Solar activity effects of ROCSAT-1 plasma density are argued to be the combined effects induced by the changes in the peak height, the scale height, and the peak electron density, respectively. Among these factors, the rise of the F_2 peak is more important for the equatorial plasma density at 600 km altitude.

Citation: Chen, Y., L. Liu, W. Wan, X. Yue, and S.-Y. Su (2009), Solar activity dependence of the topside ionosphere at low latitudes, *J. Geophys. Res.*, *114*, A08306, doi:10.1029/2008JA013957.

1. Introduction

[2] Solar EUV and X-ray radiations ionize the upper atmosphere to produce the plasma in the Earth's ionosphere. It is well known that solar radiations change over different time scales, which induces corresponding variations in the ionosphere [e.g., *Ivanov-Kholodny and Mikhailov*, 1986; *Kawamura et al.*, 2002; *Rishbeth and Garriott*, 1969]. For example, the most prominent solar cycle variation of solar radiations [e.g., *Lean et al.*, 2001; *Lundstedt et al.*, 2005] modulates significant 11-year change in the ionosphere [e.g., *Afraimovich et al.*, 2008; *Bilitza*, 2000; *Liu et al.*, 2004, 2006, 2009; *Zhao et al.*, 2005]. In addition to photoionization, the ionosphere is also controlled by recombination and dynamics processes. Thus, the study of the solar activity variations of the ionosphere is essential for understanding the changes in the ionosphere and related ionospheric processes.

[3] The daytime total electron content (TEC) tends to saturate when solar 10.7 cm radiation flux F_{107} exceeds some threshold values [e.g., *Balan et al.*, 1993, 1994a]. *Balan et al.* [1994a, 1994b] attributed the saturation effect to the nonlinear relationship of solar EUV flux with F_{107}. However, *Liu et al.* [2003] and *Liu et al.* [2006] found that the saturation effect also exists between solar EUV flux and the daytime f_oF_2 (critical frequency at the F_2 peak), or N_mF_2 (maximum electron density of the F_2 layer), and the most profound saturation effect occurs in the equatorial ionization anomaly (EIA) region. *Liu et al.* [2003] and *Liu et al.* [2006] argued that the saturation effect of N_mF_2 with F_{107} cannot simply be attributed to the nonlinear increase of EUV flux with F_{107}; ionospheric dynamics and the variations of neutral atmosphere should also play important roles. Moreover, it is interesting to note that *Liu et al.* [2009] constructed the mean TEC series from 11 years (1998–2008) of Jet Propulsion Laboratory GPS TEC data and found that an amplification effect can easily be detected in the mean TEC versus solar EUV, especially at middle and high latitudes. The amplification feature in the mean TEC is quite different from the TEC behaviors shown by *Balan et al.* [1994a].

[4] In the ionosphere, the relative importance of production, recombination, and dynamics processes should be dependent on altitude [e.g., *Ivanov-Kholodny and Mikhailov*, 1986; *Rishbeth and Garriott*, 1969]. Therefore, there may be some altitudinal dependences in the solar activity variations of the ionosphere [e.g., *L. Liu et al.*, 2007a; *Park et al.*,

[1]Beijing National Observatory of Space Environment, Institute of Geology and Geophysics, Chinese Academy of Sciences, Beijing, China.
[2]Graduate University of Chinese Academy of Sciences, Beijing, China.
[3]Institute of Space Science, National Central University, Chung-Li, Taiwan.

Copyright 2009 by the American Geophysical Union.
0148-0227/09/2008JA013957$09.00

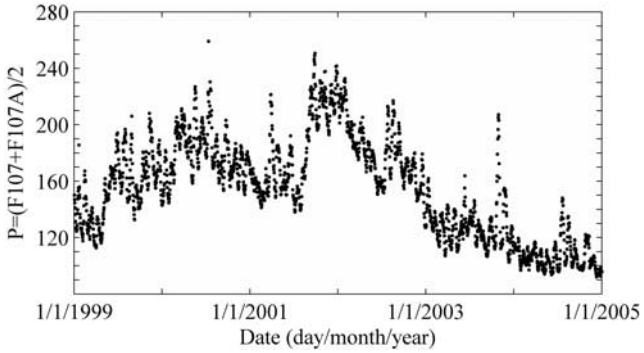

Figure 1. Solar proxy $P = (F_{107} + F_{107A})/2$ (in units of 10^{-22} W m^{-2} Hz^{-1}) from 1999 to 2004.

2008; *Y. Z. Su et al.*, 1999]. For the topside ionosphere, dynamics processes become more important. In particular, the fountain effect [e.g., *Rishbeth and Garriott*, 1969] should significantly affect the topside ionosphere in the equatorial and low latitudes. Solar activity dependences of the low-latitude ionosphere at different altitudes have been investigated with satellite observations. For example, *H. Liu et al.* [2007a] investigated the solar activity dependence of electron density at 400 km in the EIA region. With solar activity increasing, the changing rates of electron density with solar index are found to be higher in the EIA crest regions than in the trough region, which is dependent on local time and season. *L. Liu et al.* [2007a] and *Park et al.* [2008] showed that at higher solar activity levels, the topside plasma density at 840 km increases at higher rates with solar EUV flux. They proposed that this is mainly induced by the increase of the topside scale height with solar activity. In fact, some investigations have indicated a linear increase trend of the topside scale height with solar activity [e.g., *L. Liu et al.*, 2007b; *Kutiev et al.*, 2006].

[5] Previous investigations have shown that the variations of the background neutral atmosphere and dynamics processes play important roles in the solar activity dependence of the ionosphere, but the detailed ways are not quite clear. In the equatorial region, the plasma vertical drift, especially the prereversal enhancement (PRE) in the vertical drift, can significantly affect the lower topside ionosphere. Hence, it is essential to study the effects that the low-latitude ionospheric dynamics produced on the lower topside ionosphere.

[6] ROCSAT-1 observations provide a good opportunity for this study. The ROCSAT-1 satellite was launched into a low-Earth orbit on 27 January 1999. It was circulated around the Earth at altitudes of about 600 km with a 35° inclination every 97 min. The Ionospheric Plasma and Electrodynamics Instrument (IPEI) payload on ROCSAT-1 [*Chang et al.*, 1999; *S.-Y. Su et al.*, 1999; *Yeh et al.*, 1999] continuously observed the topside ion density and compositions, flow velocity, and temperatures from March 1999 to June 2004. During this period, solar activity was at moderate to high levels. The data cover all local times and geographic latitudes ±35°. Thus, it is ideal for studying the solar activity dependence of the topside ionosphere at low latitudes, especially the local time differences.

[7] In this work, solar activity dependence of the topside plasma density is investigated with the ROCSAT-1 data. Our purpose is to investigate how the equatorial dynamics processes affect the topside plasma distribution at 600 km altitude at different solar activity levels and in different local time sectors and seasons. Another purpose is to explore the variation patterns of the plasma density at 600 km with solar activity. We found profound double peaks in the topside plasma density around sunset in solar maximum equinox and December solstice months. The solar activity effects on the ROCSAT-1 plasma density are local time, seasonal, and latitudinal dependent. It is interesting that saturation effect is found in the dip equator region at equinoctial sunset, which has not been reported before. Linear and amplification trends are also detected. Thus, it is quite different from the case at higher altitudes, e.g., 800 km, where amplification trend prevails.

2. Data Analysis and Results

[8] We collected the plasma density data of the ROCSAT-1 measurements during the period from March 1999 to June 2004 to investigate the solar activity dependence of the ionosphere at 600 km altitude. The data were downloaded from the Web site http://csrsddc.csrsr.ncu.edu.tw. We divided the data into four groups, which include the data of ±45 days around the equinox or solstice day (we label them "Feb.–Apr.," "May–Jul.," "Aug.–Oct.," and "Nov.–Jan." in Figures 2–4), according to seasons. We minimize the possible geomagnetic effects by rejecting the data when the geomagnetic index $Ap > 20$.

[9] F_{107} is widely adopted as the solar proxy when continuous EUV observation is not available. Recent works have shown that there is a nonlinear relationship between solar EUV flux and F_{107} [e.g., *Balan et al.*, 1994a; *Liu et al.*, 2006; *Richards et al.*, 1994]. Meanwhile, some works [e.g., *Liu et al.*, 2006; *Richards et al.*, 1994] indicated that the index P can better represent solar EUV radiations. Therefore, we take P as the solar proxy. Figure 1 shows the P in 1999 to 2004. The F_{107} data are provided at the SPIDR Web site.

[10] We investigate the solar activity dependence of the topside ionosphere from three aspects: (1) Spatial distribution of plasma density. We investigate the solar activity effect on plasma distribution in different local time sectors and seasons. (2) Diurnal variation of plasma density. We focus on the local time variation of plasma density around sunset at different solar activity levels. (3) Solar activity variation patterns of plasma density. We investigate the patterns of the solar activity variations of plasma density in different local time sectors, seasons, and latitudes. Spring, summer, autumn, and winter are for the northern hemisphere hereinafter.

2.1. Distribution of Plasma Density

[11] The ionosphere is very dynamic at low latitudes. The equatorial fountain effect causes the well-known EIA structure, which is characterized by two off-equator peaks of plasma density in the F_2 peak region or a single peak centered close to the dip equator at higher altitudes [e.g., *Bailey et al.*, 1981; *Hanson and Moffett*, 1966; *King et al.*, 1967]. The equatorial $\mathbf{E} \times \mathbf{B}$ drift changes with local time, season, and solar activity level [e.g., *Fejer et al.*, 1991, 2008; *Scherliess and Fejer*, 1999]. So the distribution of the plasma density in the lower topside ionosphere may change

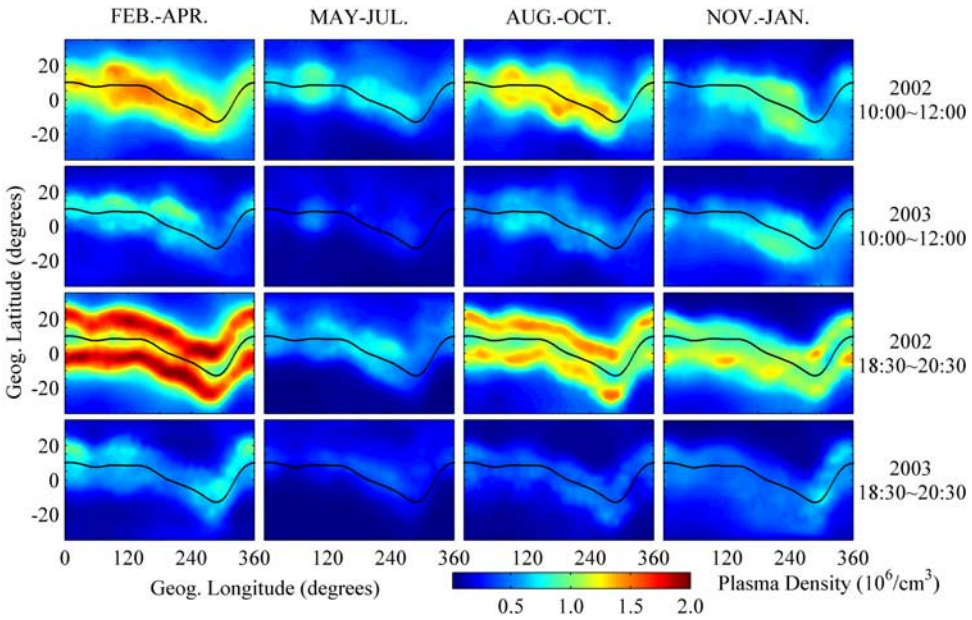

Figure 2. Spatial distribution of the plasma density observed by ROCSAT-1. Results in two local time sectors are shown: one for daytime condition (1000∼1200 LT) and the other for sunset condition (1830∼2030 LT). Year 2002 corresponds to high solar activity, and year 2003 corresponds to moderate solar activity. The black line indicates the dip equator.

over different time scales. Here we are interested in the features of the plasma distribution in different local time sectors and seasons and at different solar activity levels.

[12] We choose the data in year 2002 (solar activity is at a high level) and year 2003 (solar activity is at a moderate level) to investigate solar activity effects on the plasma density distribution. The data are averaged in bins of 4° (geographic latitude) × 30° (geographic longitude) × 2 h (local time). The plots in two local time sectors are shown in Figure 2 to highlight different effects of dynamics processes. One is for the result at 1000∼1200 LT, when the daytime upward $\mathbf{E} \times \mathbf{B}$ drift has completely developed, and the other is for the result at 1830∼2030 LT, when PRE plays an important role. In Figure 2, the distribution of plasma density is shown with a resolution of 2° in geographic latitude and 10° in geographic longitude.

[13] Around 1000∼1200 LT, the plasma density at 600 km altitude is higher in the dip equatorial region, with a peak around the dip equator. This distribution is consistent with that reported by *Chao et al.* [2004]. Here the peak is likely made up of two weak bands of higher plasma density. However, because they are close to each other, it is difficult to distinguish the density trough from these two weak peaks. We term this structure "single peak" in order to distinguish it from the profound double-peak structure. The peak is obviously enhanced at higher solar activity levels. And the distribution shows a seasonal difference. The peak is most distinct in equinoxes and more distinct in winter than in summer. Moreover, in solstices, an asymmetrical distribution about the dip equator is observed in plasma density, with higher plasma density in the summer hemisphere. The neutral wind (from the summer to the winter hemisphere) lifts the F_2 layer in the summer hemisphere and lowers it in the winter hemisphere [e.g., *Bailey and Moffett*, 1979; *Su et al.*, 1998]. Hence, the interhemisphere asymmetry is accompanied by higher h_mF_2 (peak height of the F_2 layer) and topside scale height [e.g., *Kutiev et al.*, 2006] in the summer hemisphere.

[14] We show the effects of the PRE vertical drift on the plasma distribution during 1830∼2030 LT. As can be seen in Figure 2, the single-peak structure exists at a moderate solar activity level (year 2003) during 1830∼2030 LT, and the seasonal difference and interhemisphere asymmetry in solstice seasons also can be found. At high solar activity level (year 2002), however, there are notable double peaks in equinoctial plasma density, especially in spring. There is an obvious plasma density trough at the dip equator sandwiched by two high-density bands, which nearly locate symmetrically about the dip equator. By investigating the plasma density distribution in different local time sectors and at different solar activity levels, it is found that this profound double-peak structure appears only at high solar activity level and during sunset local time sector. As for solstice seasons at high solar activity level, there is still higher plasma density around the dip equator in summer, while there are two off-equator peaks in winter, but the peak in the winter hemisphere is almost restrained except in the longitude sector with negative declinations.

2.2. Diurnal Variation

[15] Figure 3 illustrates the diurnal variation of ROCSAT-1 plasma density at two solar activity levels. According to the geomagnetic configuration, we select three latitude regions to investigate the effects of equatorial dynamics. These three regions are the dip equatorial region and the northern (southern) latitude band around 30° dip (−30° dip). The latter two correspond to the northern (southern) peak of the double-peak structure. We focus on the local time variation of plasma density around sunset to investigate how the PRE affects the low-latitude topside

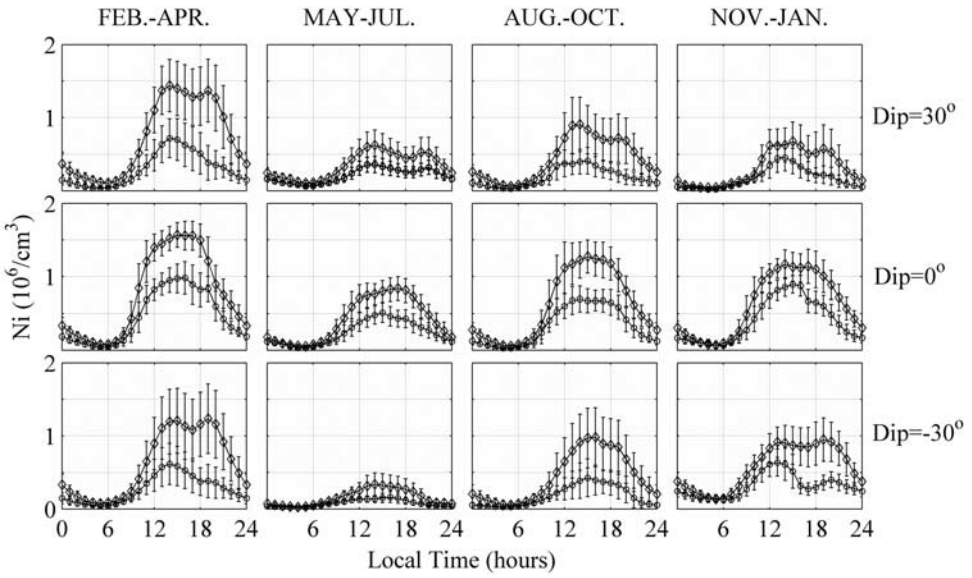

Figure 3. Diurnal variations of the plasma density observed by ROCSAT-1 in (top) the northern crest region (±2.5° around 30° dip), (middle) the dip equator region (±2.5° around 0° dip), and (bottom) the southern crest region (±2.5° around −30° dip). Data are averaged in bins of 2 h, and error bars represent standard deviations. Diamond lines correspond to high solar activity level (P = 170∼200), and circle lines correspond to moderate solar activity level (P = 120∼150).

ionosphere. The following two points are notable. (1) At lower solar activity level, the plasma density around the dip equator decreases slightly or maintains at some levels when PRE occurs, except in May–July, while it decreases with local time quickly at high solar activity level. This is most obvious in February–April. (2) At high solar activity level, the plasma density is enhanced in both off-equator bands when PRE occurs, especially in February–April. In contrast, there is no notable enhancement at lower solar activity level. The situations in May–July and in the summer hemisphere are different, and we will further mention them in section 3.

[16] There are still several interesting features in the diurnal variation of plasma density. Differences between spring and autumn can be detected in all three regions and at both solar activity levels. The plasma density is higher in spring than in autumn. Second, after sunset, the plasma density enhances in the summer hemisphere, even at lower solar activity level. Moreover, the plasma density is much higher in November–January than in May–July in the southern crest region, while in the northern crest region, the diurnal maximum of plasma density is still higher in November–January than in May–July, but the contrary is true in nighttime.

2.3. Patterns of Solar Activity Variations of Plasma Density

[17] Solar activity variations of plasma density in the topside ionosphere strongly depend on ionospheric dynamics. We explore the patterns of the variations of ROCSAT-1 plasma density with solar proxy P in different local time sectors, seasons, and dip latitudes. The result is shown in Figure 4. Two local time sectors are chosen for daytime (1000∼1200 LT) and sunset (1830∼2030 LT) conditions for the 0° dip band and the 40° dip band. The result in August–October shows quite similar patterns with that in February–April, so we just show the result in February–April and label it "Equinox." Solid lines denote quadratic regression fits of the observations, which indicate the variation trends.

[18] There are remarkable seasonal, local time, and latitudinal differences in the solar activity variations of plasma density. Three kinds of patterns are found in the variations of plasma density with P: linear, saturation, and amplification trends. During daytime, the plasma density at the dip equator increases linearly with P in all seasons. However, at the dip equator at sunset, a profound saturation trend exists in equinox seasons, and a weaker one exists in winter. No obvious saturation occurs in summer. The saturation effect always appears in the F_2 peak region. It is interesting that the saturation effect is also found at 600 km altitude. The variation trend is different in the 40° dip band. In daytime, an obvious amplification trend is found in the 40° dip band in equinox and winter, while there is a linear trend in summer. The above trends persist to sunset.

[19] The above patterns are different from the result observed by DMSP [*L. Liu et al.*, 2007a]. The DMSP plasma density always increases with solar EUV radiations at higher rates when solar activity enhances. We may also compare this result with that of *H. Liu et al.* [2007a]. They showed, during daytime, the growth rate of the plasma density at 400 km with P is higher in the EIA crest regions than that in the EIA trough region, whereas that is not true at 600-km altitude. During daytime, the rate of plasma density with P is much greater at the dip equator than that in the 40° dip band.

3. Discussion

[20] We have investigated the spatial and temporal distributions of plasma density at 600 km altitude at different

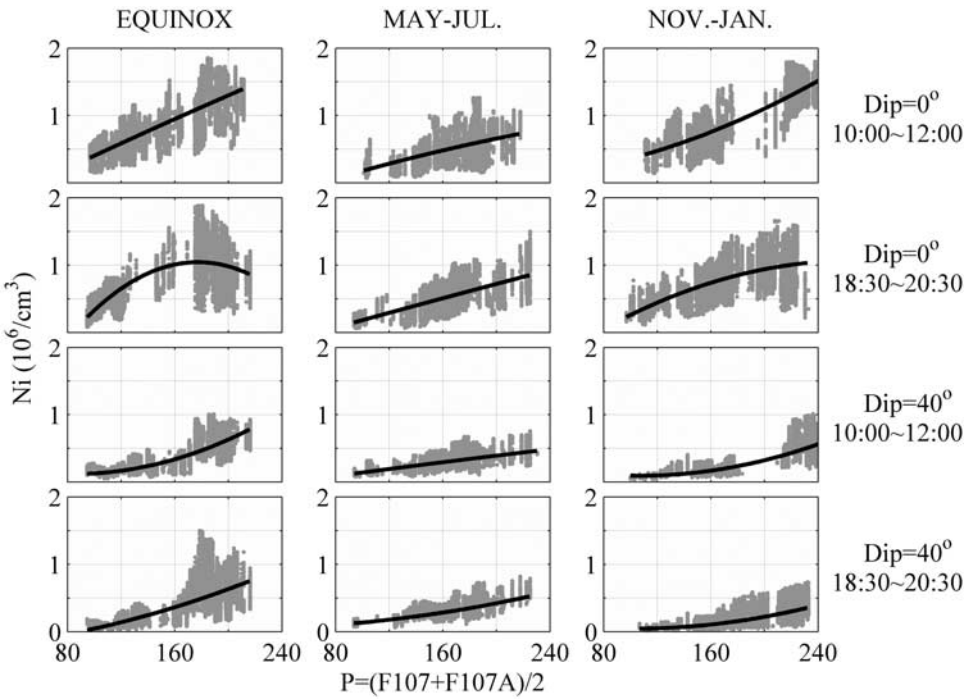

Figure 4. Solar activity variations of the topside plasma density at 600 km in the dip equatorial region (±2.5° around 0° dip) and in the 40° dip band (±2.5° around 40° dip) in selected local time sectors in three seasons. Dots denote observations, and solid lines denote quadratic regression fits.

solar activity levels. The results show significant local time, season, latitude, and solar activity differences. We may discuss these differences in terms of the variations of solar radiations, neutral atmosphere, and ionospheric dynamics.

3.1. Seasonal and Solar Activity Dependences of the Daytime Single Peak

[21] Photoionization, recombination, and dynamics processes play important roles in the F_2 peak region, while dynamics processes dominate in the topside ionosphere. During daytime, equatorial vertical drift drives the plasma to higher altitudes in the dip equator region. That enhances the peak(s) in the latitudinal distribution of plasma density in the topside ionosphere. As a result, the strength of the peak depends on the vertical drift and the plasma density in the F_2 peak region. Stronger vertical drift should induce the peak in the topside plasma density to be more distinct. The plasma density in the F_2 peak region will change when there are changes in neutral atmosphere and solar radiations. Because of the effect of the equatorial vertical drift, it is likely that the topside plasma density in the dip equator region shows stronger enhancement as compared with the case in the absence of the equatorial vertical drift.

[22] On the basis of a theoretical middle- and low-latitude ionosphere model, TIME-IGGCAS [*Yue et al.*, 2008], we modeled the increases in plasma density under two conditions: one is for 20% increase in [O], [O_2], and [N_2]; the other is for 20% increase in solar EUV radiations. Both cases enhance the photoionization in the F_2 peak region, while the recombination does not excessively enhance since [O]/[N_2] is unchanged. Our purpose is to investigate the effects of the equatorial vertical drift on the topside plasma density change when the plasma density at F_2 peak is enhanced. The model simultaneously solves the continuity, momentum, and energy equations for different ions. Three kinds of major ions (O^+, H^+, and He^+) and three kinds of minor ions (NO^+, O_2^+, and N_2^+) are included in the model. Neutral parameters are provided from the NRLMSISE00 model [*Picone et al.*, 2002] and the HWM93 model [*Hedin et al.*, 1996], and solar EUV radiations are from the EUVAC model [*Richards et al.*, 1994]. The $\mathbf{E} \times \mathbf{B}$ vertical drift, which is taken from the Fejer-Scherliess empirical drift model (F-S model) [*Scherliess and Fejer*, 1999], is considered in this model.

[23] We take F_{107} = 140, Ap = 5, and day number 80. The calculations are made at 120°E longitude. We run the model with and without the inclusion of the vertical drift. Figures 5a and 5b show the results including the F-S model drift, and Figures 5c and 5d show the results without the vertical drift. It is obvious that because of the fountain effect induced by the vertical drift, the plasma density increase is largely enhanced at some higher altitudes, but it is partly constrained in F_2 peak regions, especially near the dip equator. The enhancement is most obvious in the EIA crest regions and in the equatorial topside ionosphere (Figures 5a and 5b). Model calculations indicate that the equatorial vertical drift actually drives the plasma to higher altitudes, where recombination is slow, and then the plasma diffuses to the EIA crest regions. A considerable plasma loss is induced in the equatorial F_2 peak region, and an enhancement is produced in the equatorial topside ionosphere and the EIA crest regions. Therefore, the vertical drift partly hinders the plasma density increase in the equatorial F_2 peak region, and plasma density is much more enhanced in the equatorial topside ionosphere under the effect of the equatorial vertical drift.

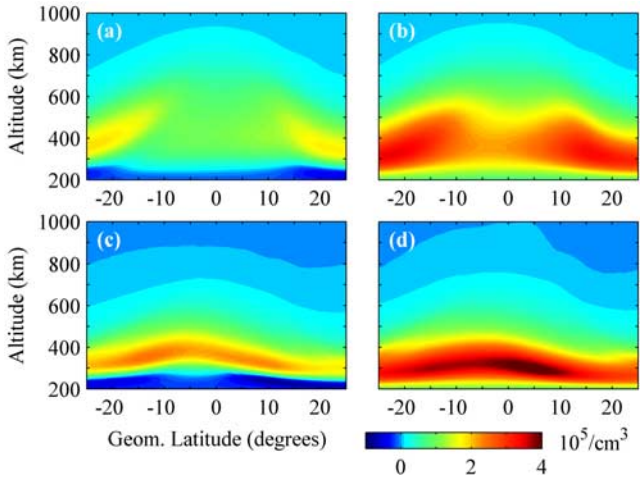

Figure 5. Simulations for the increases of the plasma density (at noontime) under two conditions: (a and c) for 20% increase in [O], [O_2], and [N_2] and (b and d) for 20% increase in solar EUV radiations. Figures 5a and 5b show results that include the **E** × **B** vertical drift effect, while Figures 5c and 5d show results that do not include the **E** × **B** vertical drift.

[24] With ROCSAT-1 observations, *Fejer et al.* [2008] found that the equatorial vertical drift in the prenoon sector is stronger in equinox and weaker in summer in most longitude sectors, and the daytime drift is nearly independent of solar activity level. Previous studies revealed that neutral density increases with solar activity and shows a semiannual variation (maxima near equinoxes and minimum near June solstice) [e.g., *Guo et al.*, 2008; *H. Liu et al.*, 2007b]. The low-latitude [O]/[N_2] at 400 km from the NRLMSISE00 model also shows a semiannual variation with maxima near equinoxes. Moreover, in the dip equatorial region, solar zenith is also slightly smaller in equinox than in solstices. Greater neutral density (as well as [O]/[N_2]) and smaller solar zenith will cause higher plasma density in the F_2 peak region in equinoxes. With the effect of the vertical drift, the topside plasma density will peak around the dip equator most distinctly in equinoxes and weakly in summer. As far as the solar activity effect is concerned, the plasma density in the F_2 peak region increases with solar activity because of enhanced EUV radiations and neutral density. In the equatorial topside ionosphere, however, the plasma density is much more enhanced under the effect of the equatorial vertical drift though it is nearly independent of solar activity level. So the topside plasma density peaks around the dip equator more distinctly at higher solar activity levels.

3.2. PRE and the Sunset Double-Peak Structure

[25] The PRE vertical drift strongly depends on solar activity level and season. It increases with solar activity, and the increase is stronger in equinoxes and weaker in summer [e.g., *Fejer et al.*, 1991, 2008; *Scherliess and Fejer*, 1999]. Around sunset, the equatorial ionosphere is primarily controlled by the PRE vertical drift in solar maximum. We first investigate the effects of PRE on the changes of equatorial plasma density at different altitudes using Jicamarca incoherent scatter radar (ISR) observations.

[26] The Jicamarca Radio Observatory is located close to the dip equator (1° dip). Figure 6 shows electron density observed by Jicamarca ISR during quiet geomagnetic periods. Figure 6 (top) plots the result in November under high

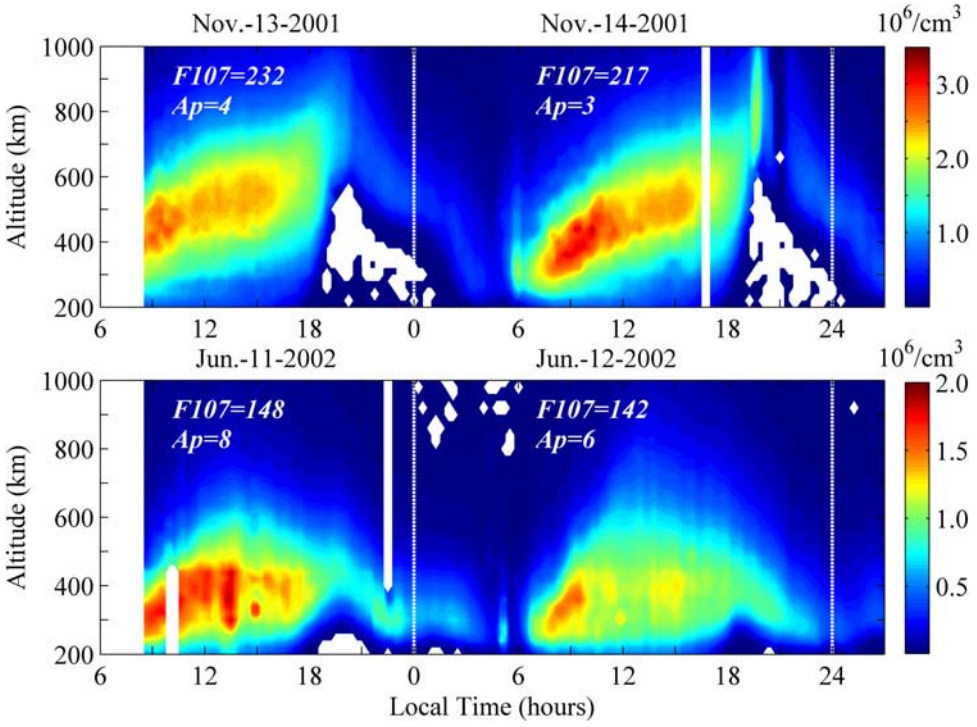

Figure 6. Electron density observed by Jicamarca incoherent scatter radar. Data are averaged in bins of 30 min (local time) × 40 km (altitude), with a resolution of 15 min in local time and 20 km in altitude.

solar activity condition, corresponding to a strong PRE, and Figure 6 (bottom) plots the result in June under moderate solar activity condition, corresponding to a weak PRE. A notable feature in Figure 6 (top) is that the F_2 layer is strongly uplifted to higher altitudes and the plasma density attenuates quickly at altitudes around the F_2 peak when PRE takes place. In contrast, the topside plasma density maintains at some levels, or even increases. In daytime, production and recombination are important; an equilibrium state develops if the drift steadies for a long time [e.g., *Rishbeth et al.*, 1978; *Woodman et al.*, 2006]. However, around sunset, the PRE vertical drift dominates over production and recombination processes, and it changes so quickly with local time that an equilibrium state cannot be reached. Thus, under the control of the PRE vertical drift, the F_2 peak is largely moved to higher altitudes [e.g., *Bertoni et al.*, 2006; *Woodman et al.*, 2006], and then the plasma diffuses along geomagnetic field lines to higher latitudes in both hemispheres. Around sunset, plasma cannot be supplied via photoionization, so the plasma density attenuates quickly at the F_2 peak altitudes but maintains at some levels or increases at higher altitudes.

[27] The profound double peaks of plasma density around sunset should be attributed to the strong fountain effect induced by the PRE vertical drift. The PRE is strongest in solar maximum equinoxes, so the fountain effect is strong and the F_2 peak can be easily lifted to high altitudes. Then, as Jicamarca ISR observations showed, the plasma density at the satellite altitude decreases quickly in the dip equator region, but it increases at both off-equator bands because of field-aligned diffusion (Figure 3). A double-peak structure develops in the topside ionosphere because of the above process. In contrast, PRE is weaker in summer or at lower solar activity levels, so the fountain effect is weaker, and the F_2 peak cannot be strongly uplifted. Now the satellite is much higher than the F_2 peak. As a consequence, the equatorial plasma density at 600 km decreases slowly with local time, or it maintains at some levels, while there are no obvious enhancements at both off-equator bands. So the double-peak structure cannot be formed.

[28] PRE is also stronger in solar maximum winter. So the double-peak structure is likely to exist. However, neutral winds also change the plasma distribution. Transequator wind affects the plasma distribution by accelerating the diffusion in the winter hemisphere and retarding the diffusion in the summer hemisphere. Meanwhile, zonal wind also contributes to field-aligned diffusion when there is a reasonable magnetic declination. In the northern hemisphere, nighttime eastward wind counteracts the effect induced by the transequator wind in the longitude sector with negative declinations, but it strengthens the transequator wind effect in the longitude sector with positive declinations [e.g., *Su et al.*, 2005]. So the peak in the northern hemisphere is restrained in the longitude sector with positive declinations, while it develops well in the longitude sector with negative declinations.

3.3. Some Questions on the Diurnal Variation of the Plasma Density

[29] We also found some interesting features in the diurnal variation of the topside plasma density. These features are also related to the variations of neutral atmosphere and the vertical drift. *H. Liu et al.* [2007b] reported two obvious asymmetries of neutral density in low-latitude regions. They are asymmetries in equinoxes (with higher values in spring) and in solstices (with higher values in December). Low-latitude [O]/[N_2] from the NRLMSISE00 model is slightly higher in spring than in autumn and much higher in winter than in summer. The equinoctial asymmetry of neutral density may lead to the asymmetry in plasma density, and the equatorial vertical drift can amplify this difference in the topside ionosphere (as shown in Figure 5). In addition, the vertical drift may be different in two equinoxes, which also can lead to the equinoctial asymmetry of the topside plasma density.

[30] In most off-equator regions, the topside plasma density is usually higher in local summer than in local winter, since the peak height and the scale height are higher in local summer. This can be found in Figure 2. It is strange that the plasma density in November–January is higher than in May–July in the northern crest region. Neutral density and [O]/[N_2] in the northern low latitudes are higher in December than in June, which may cause higher plasma density in November–January than in May–July during daytime. Moreover, the vertical drift is higher in December solstice than in June solstice according to *Fejer et al.* [2008], which also may induce higher plasma density in November–January. At night, higher peak height and scale height may lead to the topside plasma density being higher in May–July than in November–January in the northern crest region.

[31] Figure 3 shows the nighttime enhancement of plasma density in the summer hemisphere. PRE is weak at lower solar activity levels or in May–July, so it should not induce obvious enhancement of plasma density at 600 km altitude. However, the F_2 peak lifts to higher altitudes earlier in local summer because of the reversal of neutral winds before sunset [e.g., *Ivanov-Kholodny and Mikhailov*, 1986], and solar radiations can last longer in summer. Both are responsible for higher N_mF_2 in summer evening hours and should induce the enhancement of the plasma density at some altitudes above the F_2 peak.

3.4. Solar Activity Variation Trend of the Topside Plasma Density

[32] Solar activity dependence of the ionosphere is strongly related to the changes in photoionization, neutral atmosphere, and dynamics processes. The topside plasma density closely depends on N_mF_2 and h_mF_2 as well as the altitudinal distribution of the plasma density above the F_2 peak, which is primarily affected by diffusion, drifts induced by thermal winds and electric fields, and the change of the ion components. The Chapman-α function (equation (1)) is a good approximation of the topside plasma density for the steady ionosphere [e.g., *Fox*, 1994; *Lei et al.*, 2005].

$$N_i(h) = N_mF_2 \exp[0.5(1 - z - e^{-z})]$$
$$z = \frac{h - h_mF_2}{H(h)} \quad (1)$$

Here H is the effective scale height, and generally it does not equal the plasma scale height [*L. Liu et al.*, 2007b]. We discuss the solar activity variation of the topside plasma

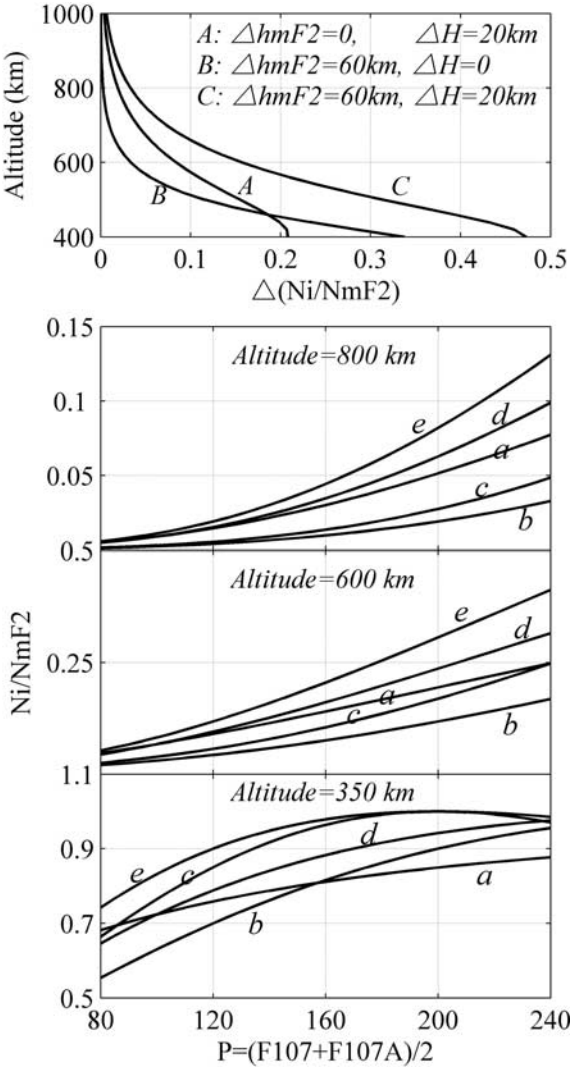

Figure 7. Results calculated with the Chapman-α function. (top) Altitudinal changes of $\Delta(N_i(h)/N_mF_2)$ for different combinations of (Δh_mF_2, ΔH) (see Table 1). (bottom) Solar activity variations of $N_i(h)/N_mF_2$ at three altitudes for different combinations of [$h_mF_2(P)$, $H(P)$] (see Table 1).

density qualitatively as done by *L. Liu et al.* [2007a]. For simplicity, we assume H is independent of altitudes. N_mF_2 saturates at high solar activity level during daytime, while the patterns of its variations with solar activity are seasonal dependent in nighttime [*Chen et al.*, 2008]. Hence the behavior of N_mF_2 is complicated, and it affects the topside plasma density linearly according to equation (1). So we first discuss what effects the changes of h_mF_2 and H produce for the topside plasma density.

[33] A parameter K is introduced into the Chapman-α function:

$$K(h,P)=\frac{N_i(h,P)}{N_mF_2(P)}=\exp\left[0.5\left(1-z(h,P)-e^{-z(h,P)}\right)\right]$$
$$z(h,P)=\frac{h-h_mF_2(P)}{H(P)} \quad (2)$$

Solar proxy P is included to show solar activity effects. Figure 7 (first panel) shows the response of plasma density at different altitudes to h_mF_2 and H increase, which is calculated according to equation (2). The changes of both h_mF_2 and H are important for plasma density at lower altitudes, while the effects of H dominate at high altitudes. And the rise of the F_2 peak can largely enhance the effect induced by the change of the scale height at high altitudes.

[34] We calculate K for different P values on the assumption that h_mF_2 and H increase linearly with P. This assumption is true on the whole [e.g., *Lei et al.*, 2005; *Liu et al.*, 2006; *Y. Z. Su et al.*, 1999]. We take five different combinations of h_mF_2 and H (see Table 1) and calculate K at three altitudes. As Figure 7 (second and third panels) shows, the variation trend is altitudinal dependent. There is an amplification trend at high altitudes (800 km) and a linear or slight amplification trend at lower altitudes (600 km). The increase of H is responsible for the amplification trend at high altitudes (800 km, line a), and the change rate of H with P determines the extent of the amplification; furthermore, the rise of the F_2 peak enhances the amplification effect. At lower altitudes (600 km), the variation trend largely depends on the change rates of h_mF_2 and H with P.

[35] The change of N_mF_2 with solar activity likewise affects the solar activity variation trend of the topside plasma density. This effect should be weak if K shows obvious amplification trend. That corresponds to the case at high altitudes [e.g., *L. Liu et al.*, 2007a; *Park et al.*, 2008]. At lower altitudes, both linear trend and amplification trend should be possible when the change of N_mF_2 is significant. That depends on the changes of K and N_mF_2 with P. Moreover, as far as a fixed altitude is concerned, its position in the topside ionosphere (at lower topside ionosphere altitude or at higher topside ionosphere altitude) rests with the F_2 peak height. Thus the rise of the F_2 peak due to the fountain effect in the dip equator region should be important.

[36] The ROCSAT-1 satellite is at lower topside ionosphere altitudes. Solar activity variation trend of ROCSAT-1 plasma density does not only depend on the change of the scale height, but also depends on the changes of h_mF_2 and N_mF_2 with solar activity. All these factors are remarkably local time, season, and latitude dependent. Therefore, solar activity variation trend of ROCSAT-1 plasma density presents seasonal, local time, and latitudinal differences.

3.5. Saturation Effect in the Topside Ionosphere

[37] Since N_mF_2 saturates at higher solar activity levels, the plasma density at a fixed altitude close to the F_2 peak will not significantly increase when solar activity enhances. So the saturation effect occurs at altitudes not far away from

Table 1. Different Combinations of h_mF_2 and H[a]

	h_mF_2 (km)	H (km)
A	280→280	40→60
B	280→340	40→40
C	280→340	40→60
a	280	0.25P+25
b	0.3P+250	0.15P+25
c	0.5P+250	0.15P+25
d	0.3P+250	0.25P+25
e	0.5P+250	0.25P+25

[a] P is in units of 10^{-22} W m^{-2} Hz^{-1}.

the F_2 peak (Figure 7, fourth panel). In the dip equator region, the F_2 peak is raised up under the effect of the PRE vertical drift. The plasma density at 600 km altitude will increase at lower solar activity levels because of the rise of the F_2 peak. In solar maximum, the F_2 peak is very high, close to or even above the satellite, under the effect of the increased PRE vertical drift. Thus plasma density at 600 km will increase no more, or even turn to decrease, when solar activity enhances. Furthermore, field-aligned diffusion, together with the lack of photoionization, will strongly decrease the plasma density in the F_2 peak region when the peak is uplifted to high altitudes. That is also important for the saturation effect.

[38] PRE is strong in equinox and weak in summer, and solar activity dependence of PRE is also seasonal dependent [e.g., *Fejer et al.*, 1991]. Thus a profound saturation effect can be detected in the solar activity dependence of ROCSAT-1 plasma density in equinoxes, and the saturation effect is weaker in winter, but it is nearly absent in summer.

4. Summary

[39] We investigated the distribution of the topside plasma density at low latitudes using ROCSAT-1 observations. The distribution feature of the plasma density at 600 km altitude varies with solar activity level, local time, and season. Plasma density peaks around the dip equator in the prenoon sector (1000∼1200 LT). This peak is most distinct in equinoxes and weaker in May–July, and it is obviously enhanced at high solar activity level. Around sunset, the latitudinal distribution of plasma density still shows a single peak structure under moderate solar activity condition, while for solar maximum, two off-equator peaks are distinct in equinox months, weak in November–January, and nearly absent in May–July.

[40] Seasonal variations of neutral density and $\mathbf{E} \times \mathbf{B}$ vertical drift can reasonably explain the seasonal feature of the prenoon peak. Higher neutral density (as well as $[O]/[N_2]$) and vertical drift cause more distinct peak in equinoxes. With the effect of the equatorial vertical drift, the plasma density is much more enhanced in the equatorial topside ionosphere when solar activity enhances. That results in the enhancement of the prenoon peak with solar activity. The local time dependence of the plasma density distribution is attributed to the local time difference of the equatorial vertical drift. The obvious double-peak structure is caused by strong PRE vertical drift. Solar activity and seasonal dependences of the plasma density distribution around sunset are due to the changes in the PRE vertical drift with solar activity level and season. In addition, neutral winds are also important for the plasma density distribution. In solar maximum, neutral winds largely restrain the northern peak of plasma density at November–January sunset.

[41] The pattern in the variations of plasma density with P shows local time, seasonal, and latitudinal differences. Three kinds of patterns (linear, amplification, and saturation) exist in the plasma density at 600 km. Saturation effect is found at the dip equator at equinoctial sunset. This saturation effect is related to the increase of PRE with solar activity. In solar maximum, strong PRE vertical drift can uplift the F_2 peak toward or even above the satellite altitude at high solar activity level, and field-aligned diffusion strongly decreases the plasma density in the F_2 peak region. These will hinder the increase of the plasma density at 600 km altitude, and the saturation effect will occur. At high altitudes, the influence induced by the change of the scale height is dominant. As a result, the amplification pattern will occur. However, the patterns in solar activity variations of ROCSAT-1 plasma density depend on the changes of the scale height as well as h_mF_2 and N_mF_2. In addition, the rise of the F_2 peak due to the equatorial vertical drift is important in the dip equator region.

[42] **Acknowledgments.** ROCSAT-1 data are downloaded from the Web site http://csrsddc.csrsr.ncu.edu.tw, and F_{107} data are from the SPIDR Web site. The Jicamarca Radio Observatory is a facility of the Instituto Geofísico del Perú operated with support from NSF cooperative agreement ATM-0432565 through Cornell University. This research was supported by National Natural Science Foundation of China (40725014, 40674090) and National Important Basic Research Project (2006CB806306).

[43] Zuyin Pu thanks the reviewers for their assistance in evaluating this paper.

References

Afraimovich, E. L., E. I. Astafyeva, A. V. Oinats, Y. V. Yasukevich, and I. V. Zhivetiev (2008), Global electron content: A new conception to track solar activity, *Ann. Geophys.*, *26*, 335–344.

Bailey, G. J., and R. J. Moffett (1979), The topside equatorial ionosphere during daytime: Elevated plasma temperature, the transequatorial O^+ breeze and the dynamics of minor ions, *Planet. Space Sci.*, *27*, 1075–1085, doi:10.1016/0032-0633(79)90078-3.

Bailey, G. J., R. J. Footitt, and R. J. Moffett (1981), Latitudinal gradients in the electron temperature of the lower *F* region at mid to low latitudes, *Planet. Space Sci.*, *29*, 171–184, doi:10.1016/0032-0633(81)90031-3.

Balan, N., G. J. Bailey, and B. Jayachandran (1993), Ionospheric evidence for a nonlinear relationship between the solar e.u.v. 10.7 cm fluxes during an intense solar cycle, *Planet. Space Sci.*, *41*, 141–145, doi:10.1016/0032-0633(93)90043-2.

Balan, N., G. J. Bailey, B. Jenkins, P. B. Rao, and R. J. Moffett (1994a), Variations of ionospheric ionization and related solar fluxes during an intense solar cycle, *J. Geophys. Res.*, *99*, 2243–2253, doi:10.1029/93JA02099.

Balan, N., G. J. Bailey, and R. J. Moffett (1994b), Modeling studies of ionospheric variations during an intense solar cycle, *J. Geophys. Res.*, *99*, 17,467–17,475, doi:10.1029/94JA01262.

Bertoni, F., I. S. Batista, M. A. Abdu, B. W. Reinisch, and E. A. Kherani (2006), A comparison of ionospheric vertical drift velocities measured by Digisonde and incoherent scatter radar at the magnetic equator, *J. Atmos. Sol. Terr. Phys.*, *68*, 669–678, doi:10.1016/j.jastp.2006.01.002.

Bilitza, D. (2000), The importance of EUV indices for the international reference ionosphere, *Phys. Chem. Earth, Part C*, *25*, 515–521.

Chang, Y.-S., W.-L. Chiang, S.-J. Ying, B. J. Holt, C. R. Lippincott, and K.-C. Hsieh (1999), System architecture of the IPEI payload on ROCSAT-1, *Terr. Atmos. Oceanic Sci.*, *10*(IS3), suppl., 7–18.

Chao, C. K., S.-Y. Su, and H. C. Yeh (2004), Ion temperature crests and troughs in the morning sector of the low-latitude and midlatitude topside ionosphere, *J. Geophys. Res.*, *109*, A11303, doi:10.1029/2003JA010360.

Chen, Y., L. Liu, and H. Le (2008), Solar activity variations of nighttime ionospheric peak electron density, *J. Geophys. Res.*, *113*, A11306, doi:10.1029/2008JA013114.

Fejer, B. G., E. R. de Paula, S. A. González, and R. F. Woodman (1991), Average vertical and zonal F region plasma drifts over Jicamarca, *J. Geophys. Res.*, *96*, 13,901–13,906, doi:10.1029/91JA01171.

Fejer, B. G., J. W. Jensen, and S.-Y. Su (2008), Quiet time equatorial *F* region vertical plasma drift model derived from ROCSAT-1 observations, *J. Geophys. Res.*, *113*, A05304, doi:10.1029/2007JA012801.

Fox, M. W. (1994), A simple, convenient formalism for electron density profiles, *Radio Sci.*, *29*(6), 1473–1491, doi:10.1029/94RS01666.

Guo, J., W. Wan, J. M. Forbes, E. Sutton, R. S. Nerem, and S. Bruinsma (2008), Interannual and latitudinal variability of the thermosphere density annual harmonics, *J. Geophys. Res.*, *113*, A08301, doi:10.1029/2008JA013056.

Hanson, W. B., and R. J. Moffett (1966), Ionization transport effects in the equatorial *F* region, *J. Geophys. Res.*, *71*, 5559–5572.

Hedin, A. E., et al. (1996), Empirical wind model for the upper, middle and lower atmosphere, *J. Atmos. Terr. Phys.*, *58*, 1421–1447, doi:10.1016/0021-9169(95)00122-0.

Ivanov-Kholodny, G. S., and A. V. Mikhailov (1986), *The Prediction of Ionospheric Conditions*, 168 pp., Springer, New York.

Kawamura, S., N. Balan, Y. Otsuka, and S. Fukao (2002), Annual and semiannual variations of the midlatitude ionosphere under low solar activity, *J. Geophys. Res.*, *107*(A8), 1166, doi:10.1029/2001JA000267.

King, J. W., K. C. Reed, E. O. Olatunji, and A. J. Legg (1967), The behavior of topside ionosphere during storm conditions, *J. Atmos. Terr. Phys.*, *29*, 1355–1363, doi:10.1016/0021-9169(67)90225-5.

Kutiev, I. S., P. G. Marinov, and S. Watanabe (2006), Model of topside ionosphere scale height based on topside sounder data, *Adv. Space Res.*, *37*, 943–950, doi:10.1016/j.asr.2005.11.021.

Lean, J. L., O. R. White, W. C. Livingston, and J. M. Picone (2001), Variability of a composite chromospheric irradiance index during the 11-year activity cycle and over longer time periods, *J. Geophys. Res.*, *106*, 10,645–10,658, doi:10.1029/2000JA000340.

Lei, J., L. Liu, W. Wan, and S.-R. Zhang (2005), Variations of electron density based on long-term incoherent scatter radar and ionosonde measurements over Millstone Hill, *Radio Sci.*, *40*, RS2008, doi:10.1029/2004RS003106.

Liu, H., C. Stolle, M. Förster, and S. Watanabe (2007a), Solar activity dependence of the electron density in the equatorial anomaly regions observed by CHAMP, *J. Geophys. Res.*, *112*, A11311, doi:10.1029/2007JA012616.

Liu, H., H. Lühr, and S. Watanabe (2007b), Climatology of the equatorial thermospheric mass density anomaly, *J. Geophys. Res.*, *112*, A05305, doi:10.1029/2006JA012199.

Liu, J. Y., Y. I. Chen, and J. S. Lin (2003), Statistical investigation of the saturation effect in the ionospheric foF2 versus sunspot, solar radio noise, and solar EUV radiation, *J. Geophys. Res.*, *108*(A2), 1067, doi:10.1029/2001JA007543.

Liu, L., W. Wan, and B. Ning (2004), Statistical modeling of ionospheric foF2 over Wuhan, *Radio Sci.*, *39*, RS2013, doi:10.1029/2003RS003005.

Liu, L., W. Wan, B. Ning, O. M. Pirog, and V. I. Kurkin (2006), Solar activity variations of the ionospheric peak electron density, *J. Geophys. Res.*, *111*, A08304, doi:10.1029/2006JA011598.

Liu, L., W. Wan, X. Yue, B. Zhao, B. Ning, and M.-L. Zhang (2007a), The dependence of plasma density in the topside ionosphere on the solar activity level, *Ann. Geophys.*, *25*, 1337–1343.

Liu, L., H. Le, W. Wan, M. P. Sulzer, J. Lei, and M.-L. Zhang (2007b), An analysis of the scale heights in the lower topside ionosphere based on the Arecibo incoherent scatter radar measurements, *J. Geophys. Res.*, *112*, A06307, doi:10.1029/2007JA012250.

Liu, L., W. Wan, B. Ning, and M.-L. Zhang (2009), Climatology of the mean TEC derived from GPS global ionospheric maps, *J. Geophys. Res.*, *114*, A06308, doi:10.1029/2009JA014244.

Lundstedt, H., L. Liszka, and R. Lundin (2005), Solar activity explored with new wavelet methods, *Ann. Geophys.*, *23*, 1505–1511.

Park, S. M., H. Kim, S. Min, J. Park, J. H. Lee, H. Kil, L. J. Paxton, S. Y. Su, J. Lee, and K. W. Min (2008), Effects of solar activity variations on the low latitude topside nighttime ionosphere, *Adv. Space Res.*, *42*, 626–633, doi:10.1016/j.asr.2007.11.031.

Picone, J. M., A. E. Hedin, D. P. Drob, and A. C. Aikin (2002), NRLMSISE-00 empirical model of the atmosphere: Statistical comparisons and scientific issues, *J. Geophys. Res.*, *107*(A12), 1468, doi:10.1029/2002JA009430.

Richards, P. G., J. A. Fennelly, and D. G. Torr (1994), EUVAC: A solar EUV flux model for aeronomic calculations, *J. Geophys. Res.*, *99*(A5), 8981–8992, doi:10.1029/94JA00518.

Rishbeth, H., and O. K. Garriott (1969), *Introduction to Ionospheric Physics*, 331 pp., Elsevier, New York.

Rishbeth, H., S. Ganguly, and J. C. G. Walker (1978), Field-aligned and field-perpendicular velocities in the ionospheric F_2-layer, *J. Atmos. Terr. Phys.*, *40*, 767–784, doi:10.1016/0021-9169(78)90028-4.

Scherliess, L., and B. G. Fejer (1999), Radar and satellite global equatorial *F* region vertical drift model, *J. Geophys. Res.*, *104*, 6829–6842, doi:10.1029/1999JA900025.

Su, S.-Y., H. C. Yeh, R. A. Heelis, J.-M. Wu, S. C. Yang, L.-F. Lee, and H. L. Chen (1999), The ROCSAT-1 IPEI preliminary results: Low-latitude ionospheric plasma and flow variations, *Terr. Atmos. Oceanic Sci.*, *10*, 787–804.

Su, S.-Y., C. K. Chao, H. C. Yeh, and R. A. Heelis (2005), Seasonal and latitudinal distributions of the dominant light ions at 600 km topside ionosphere from 1999 to 2002, *J. Geophys. Res.*, *110*, A01302, doi:10.1029/2004JA010564.

Su, Y. Z., G. J. Bailey, and K.-I. Oyama (1998), Annual and seasonal variations in the low-latitude topside ionosphere, *Ann. Geophys.*, *16*, 974–985, doi:10.1007/s00585-998-0974-0.

Su, Y. Z., G. J. Bailey, and S. Fukao (1999), Altitude dependences in the solar activity variations of the ionospheric electron density, *J. Geophys. Res.*, *104*, 14,879–14,891, doi:10.1029/1999JA900093.

Woodman, R. F., J. L. Chau, and R. R. Ilma (2006), Comparison of ionosonde and incoherent scatter drift measurements at the magnetic equator, *Geophys. Res. Lett.*, *33*, L01103, doi:10.1029/2005GL023692.

Yeh, H. C., S. Y. Su, Y. C. Yeh, J. M. Wu, R. A. Heelis, and B. J. Holt (1999), Scientific mission of the IPEI payload onboard ROCSAT-1, *Terr. Atmos. Oceanic Sci.*, *10*(IS3), suppl., 19–42.

Yue, X., W. Wan, L. Liu, H. Le, Y. Chen, and T. Yu (2008), Development of a middle and low latitude theoretical ionospheric model and an observation system data assimilation experiment, *Chin. Sci. Bull.*, *53*(1), 94–101, doi:10.1007/s11434-007-0462-z.

Zhao, B., W. Wan, L. Liu, X. Yue, and S. Venkatraman (2005), Statistical characteristics of the total ion density in the topside ionosphere during the period 1996–2004 using empirical orthogonal function (EOF) analysis, *Ann. Geophys.*, *23*, 3615–3631.

Y. Chen, L. Liu, W. Wan, and X. Yue, Beijing National Observatory of Space Environment, Institute of Geology and Geophysics, Chinese Academy of Sciences, Beijing 100029, China. (liul@mail.iggcas.ac.cn)

S.-Y. Su, Institute of Space Science, National Central University, Chung-Li, 32054, Taiwan.